

Distinct pairing symmetries of superconductivity in infinite-layer nickelates

Zhan Wang,¹ Guang-Ming Zhang,^{2,3,*} Yi-feng Yang,^{4,5,6,†} and Fu-Chun Zhang^{1,‡}

¹*Kavli Institute for Theoretical Sciences and CAS Center for Topological Quantum Computation, University of Chinese Academy of Sciences, Beijing 100190, China*

²*State Key Laboratory of Low-Dimensional Quantum Physics and Department of Physics, Tsinghua University, Beijing 100084, China*

³*Frontier Science Center for Quantum Information, Beijing 100084, China*

⁴*Beijing National Lab for Condensed Matter Physics and Institute of Physics, Chinese Academy of Sciences, Beijing 100190, China*

⁵*School of Physical Sciences, University of Chinese Academy of Sciences, Beijing 100190, China*

⁶*Songshan Lake Materials Laboratory, Dongguan, Guangdong 523808, China*

(Dated: June 30, 2020)

We report theoretical predictions on the pairing symmetry of the newly discovered superconducting nickelate $\text{Nd}_{1-x}\text{Sr}_x\text{NiO}_2$ based on the renormalized mean-field theory for a generalized model Hamiltonian proposed in [Phys. Rev. B **101**, 020501(R)]. For practical values of the key parameters, we find a transition between a gapped ($d + is$)-wave pairing state in the small doping region to a gapless d -wave pairing state in the large doping region, accompanied by an abrupt Fermi surface change at the critical doping. Our overall phase diagram also shows the possibility of a ($d + is$)-to s -wave transition if the electron hybridization is relatively small. In either case, the low-doping ($d + is$)-wave state is a gapped superconducting state with broken time-reversal symmetry. Our results are in qualitative agreement with recent experimental observations and predict several key features to be examined in future measurements.

Introduction. -The recent discovery of superconductivity (SC) in the single crystal thin films of infinite-layer nickelates $\text{Nd}_{1-x}\text{Sr}_x\text{NiO}_2$ [1] has stimulated intensive debates on its underlying electronic structural properties and superconducting pairing symmetries [2–10]. Despite the similarities in the crystal structure and $3d^9$ configuration of the nickelate and cuprate superconductors, there are increasing evidences suggesting that these two systems might belong to different classes of unconventional SC. Earlier first-principles calculations have revealed subtle differences in their band structures [11–21]. In experiments, the parent compound NdNiO_2 displays paramagnetic metallic behavior at high temperatures with a resistivity upturn below about 70 K, showing no sign of any magnetic long-range order [22]. This is in stark contrast with the cuprates whose parent compound is a charge-transfer insulator with antiferromagnetic (AF) long-range order. As a consequence, the nickelates may be modelled as a self-doped Mott insulator with two types of charge carriers [8], with the low-temperature upturn [1, 23] arising from the Kondo coupling between low-density conduction electrons and localized Ni- $3d_{x^2-y^2}$ moments [24]. This produces both Kondo singlets (doublets) and holes moving through the lattice of otherwise nickel spin-1/2 background, suppressing the AF long-range order, and causing a phase transition to a paramagnetic metal [8]. Latest measurements [5, 25] and first-principle calculations [9, 13] confirm this scenario and reveal a special interstitial s orbital for the hybridization [9], which is missing in previous calculations.

We expect these differences to have an immediate impact on the candidate pairing mechanism. In cuprates, additional holes are doped on the oxygen sites in the

CuO_2 planes [26–29] and combine with the $3d_{x^2-y^2}$ spins of Cu-ions to form the Zhang-Rice singlets [30]. High temperature SC with robust d -wave pairing can be derived from an effective one-band t - J model [31–33]. In nickelates, Sr doping may not only introduce additional holes on the oxygen sites to form the Ni-O spin singlets or holons (a spin zero state) [3, 34], but also reduce the number of conduction electrons, thus tilting the balance between the electron and hole carriers of distinct characters. The Hall coefficient is then expected to vary gradually and change sign with doping or temperature. One thus anticipates more rich physics in the nickelate superconductors, whose pairing symmetry may be altered by the hybridization. Indeed, latest experiment has revealed a non-monotonic change of T_c in exact accordance with the sign change of the Hall coefficient [35, 36].

To further elucidate the pairing symmetry of the nickelate superconductors, we employ here the renormalized mean-field theory (RMFT) [37] and study the superconducting pairing symmetry based on a generalized K - t - J model [8] in Eq. (1) and Eq. (2). Our calculations lead to a global phase diagram depending on the hole concentration p and the conduction electron hopping (t_c/K) which controls the effective strength of the Kondo hybridization. At small doping and with reasonable choices of parameters, our calculations reveal an unusual gapped ($d + is$)-wave SC with the time-reversal symmetry breaking, which is distinctly different from the familiar cuprate superconductivity. For large doping, we find either extended s -wave pairing or pure d -wave pairing. The latter is quite robust and occupies a large region in the phase diagram. Comparison with experiment tends to favor a transition from the gapped ($d + is$)-wave to gapless d -wave

pairing states with increasing hole doping. We further predict that the SC transition is accompanied with an abrupt Fermi surface change associated with the breakdown of the Kondo hybridization, causing potentially a crossover line in the temperature-doping phase diagram as observed in recent Hall measurements [35, 36].

Model Hamiltonian and RMFT. - We start by first introducing the generalized K - t - J model for the nickelate superconductors, given by $H = H_{t-J} + H_K$. The t - J part describes the hole doped lattice of Ni $3d_{x^2-y^2}$ spins with the nearest-neighbor AF superexchange interactions,

$$H_{t-J} = - \sum_{ij\sigma} \left(t_{ij} P_G d_{i\sigma}^\dagger d_{j\sigma} P_G + \text{h.c.} \right) + J \sum_{\langle ij \rangle} S_i \cdot S_j, \quad (1)$$

where $d_{i\sigma}$ and $d_{i\sigma}^\dagger$ are the annihilation and creation operators of the Ni $3d_{x^2-y^2}$ electrons, respectively, t_{ij} is the hopping integral between site i and j , and P_G is the Gutzwiller operator to project out doubly occupied electron states on the Ni sites. For simplicity, we consider only the nearest neighbor hopping (NN) t and next-nearest neighbor (NNN) hopping t' . The AF superexchange J is induced by the O- $2p$ orbitals but greatly reduced compared to that in cuprates. The Kondo hybridization part is given by,

$$H_K = -t_c \sum_{\langle ij \rangle, \sigma} \left(c_{i\sigma}^\dagger c_{j\sigma} + \text{h.c.} \right) + \frac{K}{2} \sum_{j\alpha; \sigma\sigma'} S_j^\alpha c_{j\sigma}^\dagger \tau_{\sigma\sigma'}^\alpha c_{j\sigma'}, \quad (2)$$

where $c_{i\sigma}$ ($c_{i\sigma}^\dagger$) are the annihilation (creation) operators of the conduction electrons from Nd $5d$, interstitial s , or other extended orbitals, t_c describes the effective hopping amplitude of the conduction electrons projected on the square lattice sites of the Ni^{1+} ions, τ^α ($\alpha = x, y, z$) are the spin-1/2 Pauli matrices, and K is the effective Kondo exchange coupling.

In the parent compounds LnNiO_2 ($\text{Ln} = \text{Nd, La, Pr}$), the total electron density ($n_c + n_d$) is one per unit cell, hence the total holon density $n_h = n_c$. For Sr doped compounds, the hole doping $p = n_h - n_c > 0$. Analyses of the Hall coefficients at high temperatures suggest that the average number of the conduction electrons is always small, i.e., $n_c = N^{-1} \sum_{j\sigma} \langle c_{j\sigma}^\dagger c_{j\sigma} \rangle \ll 1$, where N is the total number of the lattice sites.

For the RMFT calculations, the Gutzwiller renormalization factor should be included to approximate the projection operator that projects out the doubly occupied states. We have $g_t = n_h/(1 + n_h)$ for the constraint electron hopping t and t' , $g_J = 4/(1 + n_h)^2$ for the AF Heisenberg exchange J , and $g_K = 2/(1 + n_h)$ for the Kondo exchange coupling K . Four different mean-field order parameters are then introduced to decouple the quartic AF Heisenberg spin exchange and the Kondo

exchange interactions:

$$\begin{aligned} \chi_{ij} &= \langle d_{i\uparrow}^\dagger d_{j\uparrow} + d_{i\downarrow}^\dagger d_{j\downarrow} \rangle, & B &= \frac{1}{\sqrt{2}} \langle d_{j\uparrow}^\dagger c_{j\downarrow}^\dagger - d_{j\downarrow}^\dagger c_{j\uparrow}^\dagger \rangle, \\ \Delta_{ij} &= \langle d_{i\uparrow}^\dagger d_{j\downarrow}^\dagger - d_{i\downarrow}^\dagger d_{j\uparrow}^\dagger \rangle, & D &= \frac{1}{\sqrt{2}} \langle c_{j\uparrow}^\dagger d_{j\uparrow} + c_{j\downarrow}^\dagger d_{j\downarrow} \rangle. \end{aligned}$$

The resulting mean-field Hamiltonian has a bilinear form and can be expressed in the momentum space,

$$\mathcal{H}_{\text{mf}} = \sum_{\mathbf{k}} \Psi_{\mathbf{k}}^\dagger \begin{pmatrix} \chi(\mathbf{k}) & K_D & \Delta^*(\mathbf{k}) & K_B^* \\ K_D^* & \epsilon_c(\mathbf{k}) & K_B^* & 0 \\ \Delta(-\mathbf{k}) & K_B & -\chi(-\mathbf{k}) & -K_D^* \\ K_B & 0 & -K_D & -\epsilon_c(-\mathbf{k}) \end{pmatrix} \Psi_{\mathbf{k}},$$

where the Nambu spinors are defined as $\Psi_{\mathbf{k}}^\dagger = (d_{\mathbf{k}\uparrow}^\dagger, c_{\mathbf{k}\uparrow}^\dagger, d_{-\mathbf{k}\downarrow}, c_{-\mathbf{k}\downarrow})$, and the matrix elements are

$$\begin{aligned} \chi(\mathbf{k}) &= - \sum_{\alpha} \left(t g_t + \frac{3}{8} J g_J \chi_{\alpha} \right) \cos(\mathbf{k} \cdot \alpha) \\ &\quad - t' g_t \sum_{\delta} \cos(\mathbf{k} \cdot \delta) + \mu_1, \\ \epsilon_c(\mathbf{k}) &= -t_c \sum_{\alpha} \cos(\mathbf{k} \cdot \alpha) + \mu_2, \\ \Delta(\mathbf{k}) &= -\frac{3}{8} J g_J \sum_{\alpha} \Delta_{\alpha} \cos(\mathbf{k} \cdot \alpha), \\ K_D &= -\frac{3}{4} g_K K \frac{D}{\sqrt{2}}, K_B = -\frac{3}{4} g_K K \frac{B}{\sqrt{2}}. \end{aligned} \quad (3)$$

Here α denotes the vectors of the NN lattice sites and δ stands for those of the NNN sites. μ_1 and μ_2 are the chemical potentials fixing the numbers of the constraint electrons $d_{i\sigma}$ and conduction electrons $c_{i\sigma}$, respectively.

The above mean-field Hamiltonian can be diagonalized using the Bogoliubov transformation, $(d_{\mathbf{k}\uparrow}, c_{\mathbf{k}\uparrow}, d_{-\mathbf{k}\downarrow}^\dagger, c_{-\mathbf{k}\downarrow}^\dagger)^T = U_{\mathbf{k}} (\alpha_{\mathbf{k}\uparrow}, \beta_{\mathbf{k}\uparrow}, \alpha_{-\mathbf{k}\downarrow}^\dagger, \beta_{-\mathbf{k}\downarrow}^\dagger)^T$. The ground state is given by the vacuum of the Bogoliubov quasiparticles $\{\alpha_{\mathbf{k}\sigma}^\dagger, \beta_{\mathbf{k}\sigma}^\dagger\}$, which in turn yields the self-consistent mean-field equations:

$$\begin{aligned} B &= \frac{1}{\sqrt{2}N} \sum_{\mathbf{k}} (u_{13}^* u_{43}^{\mathbf{k}} + u_{14}^* u_{44}^{\mathbf{k}} - u_{21}^* u_{31}^{\mathbf{k}} - u_{22}^* u_{32}^{\mathbf{k}}), \\ D &= \frac{1}{\sqrt{2}N} \sum_{\mathbf{k}} (u_{23}^* u_{13}^{\mathbf{k}} + u_{24}^* u_{14}^{\mathbf{k}} + u_{31}^* u_{41}^{\mathbf{k}} + u_{32}^* u_{42}^{\mathbf{k}}), \\ \chi_{\alpha} &= \frac{2}{N} \sum_{\mathbf{k}} \exp[i\mathbf{k} \cdot \alpha] (u_{13}^* u_{13}^{\mathbf{k}} + u_{14}^* u_{14}^{\mathbf{k}}), \\ \Delta_{\alpha} &= \frac{2}{N} \sum_{\mathbf{k}} \exp[i\mathbf{k} \cdot \alpha] (u_{13}^* u_{33}^{\mathbf{k}} + u_{14}^* u_{34}^{\mathbf{k}}), \\ n_c &= \frac{1}{N} \sum_{\mathbf{k}} (u_{23}^{\mathbf{k}} u_{23}^* + u_{24}^{\mathbf{k}} u_{24}^* + u_{41}^{\mathbf{k}} u_{41}^* + u_{42}^{\mathbf{k}} u_{42}^*), \\ 1 - n_h &= \frac{1}{N} \sum_{\mathbf{k}} (u_{13}^{\mathbf{k}} u_{13}^* + u_{14}^{\mathbf{k}} u_{14}^* + u_{31}^{\mathbf{k}} u_{31}^* + u_{32}^{\mathbf{k}} u_{32}^*), \end{aligned} \quad (4)$$

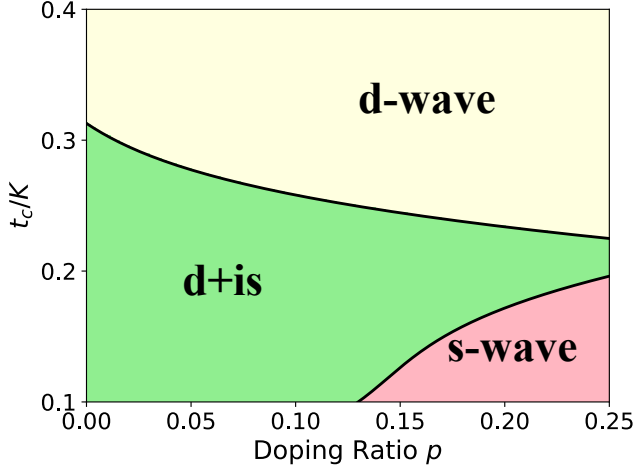


FIG. 1: Theoretical phase diagram of the superconductivity with varying hopping t_c/K and hole concentration p . At small doping, the pairing symmetry is primarily $(d + is)$ -wave SC. At large doping, the pairing is either s -wave SC for small t_c/K or d -wave SC for large t_c/K .

where $u_{ij}^{\mathbf{k}}$ are given by the matrix elements of $U_{\mathbf{k}}$, and the last two equations fix the chemical potentials μ_1 and μ_2 , respectively.

Numerical results. -For clarity, we define $\Delta_s = |\Delta_x + \Delta_y|/2$ and $\Delta_d = |\Delta_x - \Delta_y|/2$ to represent the s and d -wave pairing amplitudes, respectively. To numerically solve these self-consistent equations, we first fix the practical parameters based roughly on the experimental analyses and first-principle results. The Kondo coupling K is considered to be the largest energy scale and thus chosen as the energy unit ($K = 1$). To simplify the discussions, only the numerical results for the NN hopping $t = 0.2$, the NNN hopping $t' = -0.05$, and the AF Heisenberg spin exchange $J = 0.1$ are presented. The density of the conduction electrons is set to $n_c = 0.1$. These parameters may vary among different systems but the qualitative physical features will not be changed.

First of all, the overall phase diagram is displayed in Fig. 1 with the values of t_c/K and the hole concentration p . We find a dominant d -wave pairing symmetry in the phase diagram, which, for small t_c/K and large doping, turns into an extended s -wave state. Most intriguingly, we find a large region of the $(d + is)$ -wave pairing for small hole doping. This exotic pairing state breaks the time-reversal symmetry and its presence reflects a unique feature of the nickelate superconductivity due to the interplay of the Kondo and Mott physics in comparison with the cuprates.

Details on the transition from the mixed $(d + is)$ -wave SC to the pure d -wave SC can be found in Fig. 2(a) for an intermediate $t_c/K = 0.25$. The critical hole doping is $p^* \approx 0.13$, which is comparable with the experiment but may vary with t_c and other controlling parameters. The

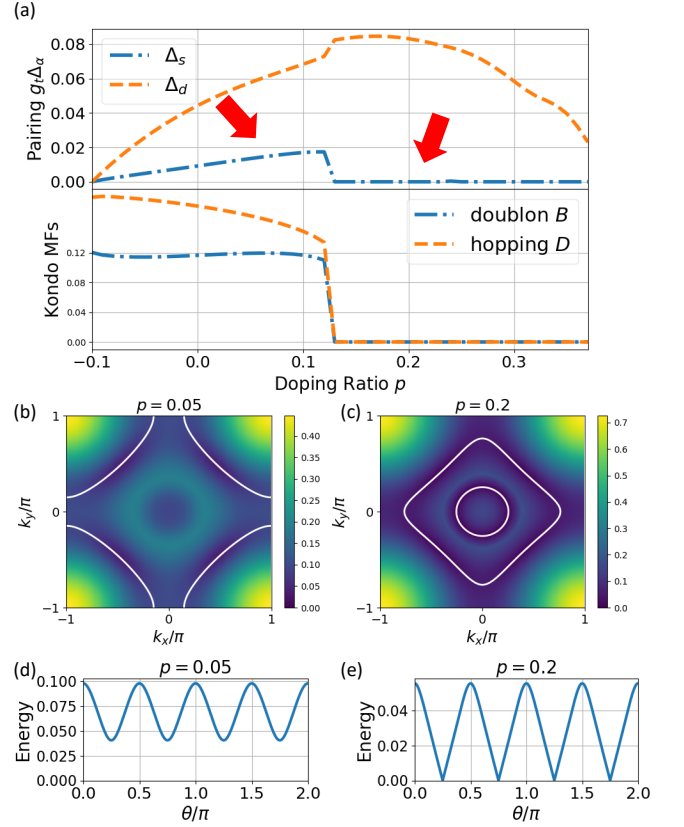


FIG. 2: RMFT results for $t_c/K = 0.25$. (a) The mean-field parameters as a function of doping for $g_t \Delta$ (upper panel) and B and D (lower panel). (b) and (c) show the quasiparticle excitation energy (background) and the Fermi surface (white solid line) defined as the minimal excitation energy at $p = 0.05$ ($d + is$)-wave and $p = 0.2$ (d -wave) as marked by the arrows in (a). (d) and (e) show the respective quasiparticle excitation gap along the Fermi surface.

transition is accompanied with vanishing Kondo mean-field parameters B and D , implying a breakdown of the Kondo hybridization in the large doping side. It also implies that the s -wave component is primarily associated with the Kondo hybridization effect and the d -wave component is from the usual t - J model. The corresponding Fermi surface structures in these two different doping regions can be extracted from the minimal energy contour of the SC quasiparticle excitation energy. Two typical dopings for $p = 0.05$ and $p = 0.2$ are plotted in Figs. 2(b) and 2(c), and the corresponding SC gap functions are plotted in Figs. 2(d) and 2(e). For small doping $p < p^*$, the normal state has a large hole-like Fermi surface around four Brillouin zone corners, while for large doping, two types of charge carriers are effectively decoupled and give rise to two separate electron-like Fermi surfaces around the Brillouin zone center. The physics of the pure d -wave pairing region is similar to that of heavily hole-doped cuprates for this particular doping. We have

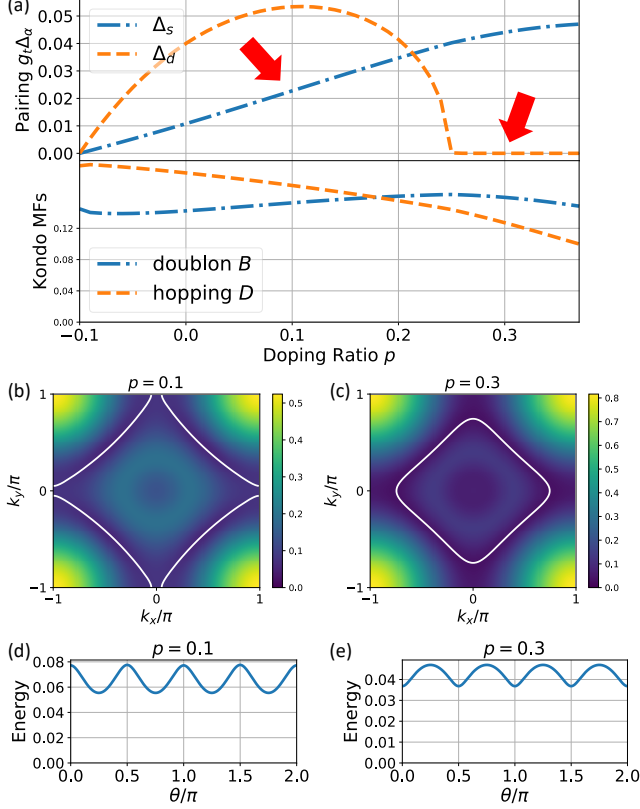


FIG. 3: RMFT results for $t_c/K = 0.2$. (a) The mean-field parameters as a function of doping for $g_t \Delta$ (upper panel) and B and D (lower panel). (b) and (c) show the quasiparticle excitation energy (background) and the Fermi surface (white solid line) at $p = 0.1$ ($d + is$ -wave) and $p = 0.3$ (s -wave) as marked by the arrows in (a). (d) and (e) show the respective quasiparticle excitation gap along the Fermi surface.

thus a concurrent Lifshitz transition at the critical hole doping p^* , accompanying the transition between different pairing states of the nickelate superconductivity.

For comparison, the RMFT results for a smaller $t_c/K = 0.2$ are also presented in Fig. 3, where the hole doping induces a transition from the ($d + is$)-wave to the pure s -wave SC. In both phases, the SC are gapped and the Kondo mean-field parameters D and B remain finite. Hence the hybridization effect is not affected across the transition. Again, the Fermi surfaces for $p = 0.1$ and $p = 0.3$ are extracted and shown in Figs. 3(b) and 3(c), respectively, with the corresponding SC gap functions displayed in Figs. 3(d) and 3(e). We still see a Lifshitz transition of the Fermi surfaces, but it is no longer associated with the breakdown of the hybridization but a pure doping effect as in cuprates.

Discussions and Conclusion. -The generalized K - t - J model contains several key energy scales that need to be fixed for better experimental comparison in each individual compound. While the conduction electron hopping

t_c may be roughly estimated from band calculations, the constraint electron hoppings t and t' are strongly renormalized due to the background AF correlations. Following our previous analyses, the Heisenberg superexchange J is expected to be roughly the order of 10-100 meV, which is smaller than that of cuprates due to the larger charge transfer energy between O-2 p and Ni-3 $d_{x^2-y^2}$ orbitals. The Kondo exchange interaction K is estimated to be the order of 100-1000 meV [8, 9]. This justifies our choice of J/K in current numerical calculations. In any case, our results may serve as a qualitative guide for future studies on nickelate superconductors.

It is worthwhile comparing our results with the available experiment. Recent systematic measurements on the resistivity and Hall coefficients in $\text{Nd}_{1-x}\text{Sr}_x\text{NiO}_2$ have revealed a non-monotonic doping dependence of the superconducting T_c , whose local minimum coincides with the sign change of the Hall coefficient [35, 36]. The latter further gives rise to a crossover line in the temperature-doping phase diagram of the nickelate superconductors. A straightforward comparison suggests that the experimental observation may correspond to our derived transition from the ($d + is$)-wave pairing to the d -wave or s -wave pairing. The concurrent change in the Hall coefficient therefore marks a potential Fermi surface change, in resemblance of that observed in some heavy fermion systems owing to the breakdown of the Kondo hybridization [38]. The latter also leads to a delocalization line in the temperature-pressure or temperature-doping phase diagram [39]. It is thus attempted to link the experiment with our theoretical proposals, predicting the SC transition from a gapped ($d + is$)-wave state to a gapless d -wave pairing state, with the crossover line in the temperature-doping plane potentially associated with the Fermi surface change due to the Kondo hybridization.

If this is the case, one may further expect several key features to be examined in future experiment: 1) a superconducting transition between gapped and gapless pairings with increasing doping to be best revealed by the scanning tunneling spectroscopy or the penetration depth measurement; 2) time-reversal symmetry breaking in the low-doping gapped SC phase to be detected in the μSR or Kerr experiments; 3) Fermi surface reconstruction accompanying the superconducting transition to be measured by the quantum oscillation experiments or angle-resolved photoemission spectroscopy. Additionally, there may also exist other exotic properties associated with the quantum critical point, besides the non-Fermi liquid behavior which has been observed in superconducting nickelate thin films with $\rho \sim T^\alpha$ and $\alpha = 1.1 - 1.3$ [8]. It will be interesting to see if future measurements will confirm these preliminary predictions or suggest a different parameter region in our generalized model.

In conclusion, we have discussed the pairing symmetry of the newly discovered superconducting nickelate $\text{Nd}_{1-x}\text{Sr}_x\text{NiO}_2$ based on the RMFT for a generalized K -

t - J model. Our calculations reveal an interesting interplay between the Kondo and Mott physics. For practical choices of the parameters, we find a transition from a gapped ($d + is$)-wave state to a gapless d -wave state with increasing doping. An extended s -wave pairing has also been predicted but requires sufficiently small hopping and large doping. For the former transition, our calculations suggest a concurrent Fermi surface change and a corresponding crossover line in the temperature-doping phase diagram due to the breakdown of the Kondo hybridization. Our proposal is in good agreement with available experiments and gives several key predictions for further verification.

Note Added. As we are finishing this manuscript, single particle tunneling measurements [40] were reported on superconducting nickelate thin films with $T_c \approx 9.1K$, and two distinct types of tunneling spectra were revealed: a V-shape feature with a gap maximum 3.9 meV, a U-shape feature with a gap about 2.35 meV, and some spectra with mixed contributions of the two components. These spectra were ascribed to different Fermi surfaces from the conduction and Ni $3d_{x^2-y^2}$ orbitals. However, according to our present calculations, these distinct tunneling spectra observed at different locations on the thin films may be caused by different hole doping concentrations due to surface effects, so the different spectral shapes may correspond to the different pairing states in our theory. In this sense, the tunneling experiment is supportive of our theoretical prediction of multiple superconducting phases.

Acknowledgment.- This work was supported by the National Key Research and Development Program of MOST of China (2016YFYA0300300, 2017YFA0302902, 2017YFA0303103), the National Natural Science Foundation of China (11774401, 11674278), the State Key Development Program for Basic Research of China (2014CB921203 and 2015CB921303), and the Strategic Priority Research Program of CAS (Grand No. XDB28000000).

* Electronic address: gmzhang@tsinghua.edu.cn

† Electronic address: yifeng@iphy.ac.cn

‡ Electronic address: fuchun@ucas.ac.cn

- [1] D. Li, K. Lee, B. Y. Wang, M. Osada, S. Crossley, H. R. Lee, Y. Cui, Y. Hikita, and H. Y. Hwang, *Nature* **572**, 624 (2019).
- [2] A. S. Botana and M. R. Norman, *Phys. Rev. X* **10**, 011024 (2020).
- [3] M. Jiang, M. Berciu, and G. Sawatzky, *Phys. Rev. Lett.* **124**, 207004 (2020).
- [4] H. Sakakibara, H. Usui, K. Suzuki, T. Kotani, H. Aoki, and K. Kuroki, *arXiv:1909.00060* (2019).
- [5] M. Hepting, D. Li, C. J. Jia, H. Lu, E. Paris, Y. Tseng, X. Feng, M. Osada, E. Been, Y. Hikita, Y.-D. Chuang, Z. Hussain, K. J. Zhou, A. Nag, M. Garcia-Fernandez, M.

- Rossi, H. Y. Huang, D. J. Huang, Z. X. Shen, T. Schmitt, H. Y. Hwang, B. Moritz, J. Zaanen, T. P. Devereaux, and W. S. Lee, *Nature Materials* **19**, 381 (2020).
- [6] Y. Normura, M. Hirayama, T. Tadano, Y. Yoshimoto, K. Nakamura, and R. Arita, *Phys. Rev. B* **100**, 205138 (2019).
- [7] X. Wu, D. D. Sante, T. Schwemmer, W. Hanke, H. Y. Hwang, S. Raghu, and Ronny Thomale, *Phys. Rev. B* **101**, 060504 (2020).
- [8] G. M. Zhang, Y. F. Yang and F. C. Zhang, *Phys. Rev. B* **101**, 020501(R) (2020).
- [9] Y. Gu, S. Zhu, X. Wang, J. Hu, H. Chen, *Communications Physics* **3**, 84 (2020).
- [10] J. Karp, A. S. Botana, M. R. Norman, H. Park, M. Zingl, and A. Millis, *Phys. Rev. X* **10**, 021061 (2020).
- [11] V. I. Anisimov, D. Bukhvalov, and T. M. Rice, *Phys. Rev. B* **59**, 7901-7906 (1999).
- [12] M. A. Hayward, M. A. Green, M. J. Rosseinsky, and J. Sloan, *J. Am. Chem. Soc.* **121**, 8843 (1999).
- [13] K.-W. Lee and W. E. Pickett, *Phys. Rev. B* **70**, 165109 (2004).
- [14] A. S. Botana, V. Pardo, and M. R. Norman, *Phys. Rev. Materials* **1**, 021801(R) (2017).
- [15] J. Chaloupka and G. Khaliullin, *Phys. Rev. Lett.* **100**, 016404 (2008).
- [16] P. Hansmann, X. Yang, A. Toschi, G. Khaliullin, O. K. Andersen, and K. Held, *Phys. Rev. Lett.* **103**, 016401 (2009).
- [17] S. Middey, J. Chakhalian, P. Mahadevan, J. W. Freeland, A. J. Millis, and D. D. Sarma, *Annu. Rev. Mater. Res.* **46**, 305 (2016).
- [18] A. V. Boris, Y. Matiks, E. Benckiser, A. Frano, P. Popovich, V. Hinkov, P. Wochner, M. Castro-Colin, E. Detemple, V. K. Malik, C. Bernhard, T. Prokscha, A. Suter, Z. Salman, E. Morenzoni, G. Cristiani, H.-U. Habermeier, and B. Keimer, *Science* **332**, 937 (2011).
- [19] E. Benckiser, et. al., E. Benckiser, M. W. Haverkort, S. Brück, E. Goering, S. Macke, A. Frañó, X. Yang, O. K. Andersen, G. Cristiani, H.-U. Habermeier, A. V. Boris, I. Zegkinoglou, P. Wochner, H. Kim, V. Hinkov, and B. Keimer, *Nat. Mater.* **10**, 189 (2011).
- [20] A. S. Disa, D. P. Kumah, A. Malashevich, H. Chen, D. A. Arena, E. D. Specht, S. Ismail-Beigi, F. J. Walker, and C. H. Ahn, *Phys. Rev. Lett.* **114**, 026801 (2015).
- [21] J. Zhang, A. S. Botana, J. W. Freeland, D. Phelan, H. Zheng, V. Pardo, M. R. Norman, and J. F. Mitchell, *Nat. Phys.* **13**, 864 (2017).
- [22] M. A. Hayward and M. J. Rosseinsky, *Solid State Sciences* **5**, 839 (2003).
- [23] A. Ikeda, Y. Krockenberger, H. Irie, M. Naito, and H. Yamamoto, *Applied Physics Express* **9**, 061101 (2016).
- [24] Actually an alternative explanation for the resistivity upturn at low temperatures is weak localization due to the presence of disorder holes in the NiO₂ plane. It can also give rise to a logarithmic temperature dependent correction. However, the corresponding correction to the Hall coefficient is independent of temperature in the same region, which does not support this explanation.
- [25] B. H. Goodge, D. Li, M. Osada, B. Y. Wang, K. Lee, G. A. Sawatzky, H. Y. Hwang, L. F. Kourkoutis, *arXiv:2005.02847*.
- [26] J. P. Bednorz and K. A. Muller, *Z. Phys. B* **64**, 189 (1986).
- [27] P. W. Anderson, *Science* **235**, 1196 (1987).

- [28] P. W. Anderson, P. A. Lee, M. Randeria, T. M. Rice, N. Trivedi, and F. C Zhang, *J. Phys.: Condens. Matter* **16**, R755 (2004).
- [29] P. A. Lee, N. Nagaosa, and X. G. Wen, *Rev. Mod. Phys.* **78**, 17 (2006).
- [30] F. C. Zhang, and T. M. Rice, *Phys. Rev. B* **37**, 3759 (1988).
- [31] Z. X. Shen, D. S. Dessau, B. O. Wells, D. M. King, W. E. Spicer, A. J. Arko, D. Marshall, L. W. Lombardo, A. Kapitulnik, P. Dickinson, S. Doniach, J. DiCarlo, T. Loeser, and C. H. Park, *Phys. Rev. Lett.* **70**, 1553 (1993).
- [32] D. A. Wollman, D. J. Van Harlingen, W. C. Lee, D. M. Ginsberg, and A. J. Leggett, *Phys. Rev. Lett.* **71**, 2134 (1993).
- [33] C. C. Tsuei, J. R. Kirtley, C. C. Chi, L. S. Yujahnes, A. Gutpa, T. Shaw, J. Z. Sun, and M. B. Ketchen, *Phys. Rev. Lett.* **73**, 593 (1994).
- [34] Z. J. Lang, R. Jiang, and W. Ku, arXiv:2005.00022.
- [35] D. Li, B. Y. Wang, K. Lee, S. P. Harvey, M. Osada, B. H. Goodge, L. F. Kourkoutis and H. Y. Hwang, arXiv:2003.08506.
- [36] S. Zeng, C. S. Tang, X. Yin, C. Li, Z. Huang, J. Hu, W. Liu, G. J. Omar, H. Jani, Z. S. Lim, K. Han, D. Wan, P. Yang, A. T. S. Wee, A. Ariando, arXiv:2004.11281.
- [37] F. C. Zhang, C. Gros, T. M. Rice, and H. Shiba, *Supercond. Sci. Technol.* **1**, 36 (1988).
- [38] Q. Si, J. H. Pixley, E. Nica, S. J. Yamamoto, P. Goswami, R. Yu, and S. Kirchner, *J. Phys. Soc. Jpn.* **83**, 061005 (2014)
- [39] Y.-F. Yang, D. Pines, and G. Lonzarich, *Proc. Natl. Acad. Sci. USA* **114**, 6250 (2017).
- [40] Q. Gu, Y. Li, S. Wan, H. Li, W. Guo, H. Yang, Q. Li, X. Zhu, X. Pan, Y. Nie & Hai-Hu Wen, arXiv:2006.13123.